Chemical Geology 369 (2014) 12–21

Contents lists available at ScienceDirect

Chemical Geology

journal homepage: www.elsevier.com/locate/chemgeo

Quantification of the elemental incompatibility sequence, and composition of the "superchondritic" mantle

Youxue Zhang

Department of Earth and Environmental Sciences, The University of Michigan, Ann Arbor, MI 48109-1005, USA

ARTICLE INFO

Article history:
Received 11 September 2013
Received in revised form 13 January 2014
Accepted 20 January 2014
Available online 29 January 2014

Editor: K. Mezger

Keywords:
Incompatible elements
Compatibility sequence
Superchondritic mantle
Subchondritic mantle
Mantle composition

ABSTRACT

The classic compositional model for the bulk Earth and bulk silicate Earth is the "chondritic" model, in which the refractory elements in the bulk Earth, and the refractory lithophile elements in the bulk silicate Earth, are assumed to be in chondritic proportions. Recent discovery of ^{142}Nd anomalies has challenged this view and there has been discussion of a superchondritic Earth or superchondritic mantle, although an alternative explanation that the ^{142}Nd anomalies are inherited from nucleosynthetic anomaly has also been discussed. If the bulk silicate Earth is not chondritic in terms of refractory and lithophile elements, the foundation for many previous publications would be shifted and the new bulk silicate Earth composition must be estimated. This work quantifies the incompatibility sequence and shows that even if the mantle is "superchondritic", it is still quantitatively consistent with a partially depleted chondritic mantle. Normalization using chondritic mantle abundances is still appropriate. Furthermore, the major and trace lithophile elemental composition of the proposed "superchondritic" mantle as a partially depleted chondritic mantle is derived.

1. Introduction

Classically, the composition of bulk silicate Earth (BSE) and whole Earth is modeled as chondritic (e.g., Jagoutz et al., 1979; Sun, 1982; Zindler and Hart, 1986; Allegre et al., 1995; McDonough and Sun, 1995; Palme and O'Neill, 2004). Because refractory elemental ratios are essentially constant in chondrites, the chondritic model allows precise constraint of these ratios in the whole Earth and bulk silicate Earth (BSE). For BSE, siderophile and chalcophile elements are depleted due to core formation, and hence only the refractory and lithophile elements (Be, Al, Ca, Sc, Ti, V, Sr, Y, Zr, Nb, Ba, Y, REE, Hf, Ta, Th, and U, where REE means rare earth elements) are in chondritic proportions. In deriving BSE compositions, by adopting the chondritic model, the concentrations of the refractory and lithophile elements are easily determined, and those of other elements are inferred by numerous sophisticated ways (such as isotopic ratios and elemental ratios). Not only BSE and whole Earth compositions are derived using the chondritic assumption, but also rock composition data are often presented relative to chondritic BSE (hereafter referred to as C-BSE) for discussing the compositional evolution and petrogenesis.

Since 1992, high-precision ^{142}Nd/^{144}Nd data have revealed anomalies in the ratio. ^{142}Nd is the decay daughter of the extinct nuclide ^{146}Sm (half life 68 ± 7 Myr, Kinoshita et al., 2012). Hence, any anomaly in the ^{142}Nd/^{144}Nd ratio in rocks implies either very early differentiation of the Sm/Nd ratio, or a nonchondritic earth, or nucleosynthetic anomalous Nd contributing to Earth. Harper and Jacobsen (1992) reported higher ^{142}Nd/^{144}Nd ratio by about 30 ppm in 3.8-Ga Isua rocks compared to modern rocks, and inferred very early (4.44–4.54 Ga) crust–mantle differentiation (they did not propose a nonchondritic Earth). The observation was debated for some time and eventually the anomalies were confirmed although smaller than 30 ppm (Boyet et al., 2003; Caro et al., 2003; Boyet and Carlson, 2006; Caro et al., 2006). Recently, Boyet and Carlson (2005) discovered that ^{142}Nd/^{144}Nd ratio in modern terrestrial rocks is about 20 ppm higher than that in chondrites and proposed either a very early (4.53 Ga) differentiation and the presence of a hidden Earth reservoir with lower ^{142}Nd/^{144}Nd ratios, or a superchondritic Earth. Boyet and Carlson (2006) and Jackson and Carlson (2012) reported that essentially all terrestrial rocks have higher ^{142}Nd/^{144}Nd ratio than chondrites, and proposed that either the BSE is superchondritic with Sm/Nd ratio higher than chondrites by about 6% relative, or an enriched reservoir is hidden in the deep mantle. Caro et al. (2008) showed that Moon and Mars share the same superchondritic characteristics. The proposed superchondritic mantle would lead to a higher ^{143}Nd/^{144}Nd ratio than earlier estimates based on the chondritic model. This higher ^{143}Nd/^{144}Nd ratio (~0.51299) is close to the PREvalent MAntle (PREMA, Zindler and Hart, 1986) or FOZO (Hart, 1992) with low and plume-like ^{4}He/^{3}He ratios (Jackson and Jellinek, 2013). Because FOZO is defined as the common endmember of isotopic mixing trends for mid-ocean ridge basalts (hereafter MORB) sampling depleted MORB mantle (DMM hereafter) and many ocean island basalt suites sampling different heterogeneities in the mantle, the similarity between ^{143}Nd/^{144}Nd ratio in the superchondritic mantle and FOZO lends support to the superchondritic mantle hypothesis. O'Neill and Palme (2008) proposed collisional erosion of ~10% of the silicate earth (14% of which is the subchondritic protocrust) to produce a superchondritic Earth. Caro and Bourdon (2010) inferred the Lu/Hf and

0009-2541/$ – see front matter © 2014 Elsevier B.V. All rights reserved.
http://dx.doi.org/10.1016/j.chemgeo.2014.01.012

Rb/Sr ratios of the superchondritic BSE from the PREMA $^{143}Nd/^{144}Nd$ ratio using $^{176}Hf/^{177}Hf$ versus $^{143}Nd/^{144}Nd$ trend and $^{87}Sr/^{86}Sr$ versus $^{143}Nd/^{144}Nd$ trend. Jackson and Jellinek (2013) equated superchondritic mantle (hereafter SCM) to be the low-$^4He/^3He$ mantle, estimated its composition, and discussed implications for a nonchondritic Earth. On the other hand, Huang et al. (2013) re-evaluated the superchondritic mantle claim, arguing that even though chondrites are very homogeneous in Sm/Nd ratio (Sm/Nd mass ratio of 0.3254 ± 0.0056, 1.7% relative error), the $^{142}Nd/^{144}Nd$ ratio in chondrites is variable with total variation of about 50 ppm due to nucleosynthetic anomalies (Andreasen and Sharma, 2006; Carlson et al., 2007; Gannoun et al., 2011), making it difficult to use the 20-ppm difference to argue for a superchondritic Earth. In addition, Javoy (1995) and Javoy et al. (2010) proposed an enstatite chondrite model for Earth based on isotopic similarities, and terrestrial $^{142}Nd/^{144}Nd$ ratios fall within the range of enstatite chondrites (Huang et al., 2013), further supporting the enstatite chondrite model, although debate on the enstatite chondrite model is also intense (e.g., Rubie et al., 2011; Fitoussi and Bourdon, 2012; Zambardi et al., 2013). In summary, three explanations have been advanced for the observed high $^{142}Nd/^{144}Nd$ ratios in terrestrial rocks than in ordinary and carbonaceous chondrites: (1) The high $^{142}Nd/^{144}Nd$ ratios are of nucleosynthetic origin and Earth accumulated chondritic Sm/Nd ratios. Hence, we can still use chondritic models. (2) The high $^{142}Nd/^{144}Nd$ ratios are not a whole mantle signature, but a signature due to early differentiation, which removed a subchondritic early enriched reservoir (EER) that was either hidden (e.g., in D″ layer) or lost by impacts, so that the rocks that can be observed today are from the complementary superchondritic early depleted reservoir (EDR). In the impact loss version, the whole Earth is superchondritic. (3) Earth accreted from superchondritic materials. In this scenario, it is not clear whether or not the SCM composition can be related to C-BSE. The debate is continuing.

If Earth's mantle is superchondritic, previous estimates of BSE composition and related work (many papers!) must be reevaluated without using the assumption of chondritic refractory and lithophile elemental ratios. This would change the concentrations of not only the refractory lithophile elements, but also other elements because the concentrations of the other elements are often derived by using ratios to some refractory lithophile elements (e.g., K concentration is derived from K/U ratio, and Rb concentration is derived from Rb/Sr). Can the composition of SCM be quantitatively related to C-BSE by depletion through mantle partial melting? Can C-BSE still be used as the reference composition? Boyet and Carlson (2006) discussed various scenarios, including one in which SCM is partially depleted mantle. However, they didn't demonstrate this in a quantitative and rigorous way. On the other hand, O'Neill and Palme (2008) and Campbell and O'Neill (2012) argued that the whole Earth itself is superchondritic due to impact loss of subchondritic material. Caro and Bourdon (2010) stated that the superchondritic mantle contradicts the long-held view that chondrites represent a reference composition for the ^{147}Sm–^{143}Nd system.

The goal of this work is to explore whether the SCM and DMM are related to C-BSE by different degrees of depletion using Sm/Nd, Lu/Hf and Rb/Sr ratios previously inferred for SCM (Boyet and Carlson, 2006; Caro and Bourdon, 2010). I quantify the sequence of incompatible elements, show that SCM is compositionally related to C-BSE and DMM, and use the relation to derive internally consistent SCM composition. That is, it does not look like that Earth accreted from superchondritic materials. Even if Earth's mantle is superchondritic either because of a hidden subchondritic reservoir, or because of impact loss of subchondritic materials, it is still appropriate to use the chondritic model as the reference or normalizing composition, and previous work on mantle composition and igneous rock evolution based on the chondritic mantle does not have to be revisited.

Various authors estimated C-BSE compositions (e.g., Jagoutz et al., 1979; Sun, 1982; Zindler and Hart, 1986; Allegre et al., 1995; McDonough and Sun, 1995; Palme and O'Neill, 2004; Lyubetskaya and Korenaga, 2007). The differences among these estimates are usually small. For example, the concentrations of lithophile trace elements in Palme and O'Neill (2004) are on average higher by 4% relative than those in McDonough and Sun (1995). However, the estimates by Lyubetskaya and Korenaga (2007) of concentrations of lithophile trace elements are lower than those by McDonough and Sun (1995) by about 20% on average. On the other hand, the lithophile trace elemental ratios are more or less the same in different estimates. In this work, the C-BSE data by McDonough and Sun (1995) will be used as the reference C-BSE composition to evaluate the relation between SCM and DMM compositions and to obtain SCM composition for internal consistency because DMM compositions are obtained relative to this C-BSE (e.g., Table 4 of Salters and Stracke, 2004; and Fig. 2 of Workman and Hart, 2005). The McDonough and Sun (1995) paper will be referred as MS1995, Salters and Stracke (2004) as SS2004, and Workman and Hart (2005) as WH2005.

2. Isotopic and elemental constraints of SCM

The "superchondritic" mantle is essentially defined by the necessary Sm/Nd ratio to produce $^{142}Nd/^{144}Nd$ ratio that is 0.18 epsilon units above that of chondrites (Boyet and Carlson, 2005, 2006; Caro and Bourdon, 2010). The higher-than-chondritic $^{142}Nd/^{144}Nd$ ratio leads to a higher-than-chondritic $^{143}Nd/^{144}Nd$ isotopic ratio in the mantle, which falls in the region of PREMA (Zindler and Hart, 1986) or FOZO (Hart, 1992). Furthermore, knowing the $^{143}Nd/^{144}Nd$ ratio in SCM means that $^{176}Hf/^{177}Hf$ ratio in SCM can be inferred from the Hf–Nd isotopic array for mantle samples (Blichert-Toft and Albarede, 1997; Vervoort et al., 1999; Caro and Bourdon, 2010), and $^{87}Sr/^{86}Sr$ ratio in SCM can be inferred from the Nd–Sr isotopic array (Zindler and Hart, 1986; Jackson et al., 2007; Caro and Bourdon, 2010). From the estimated $^{176}Hf/^{177}Hf$ and $^{87}Sr/^{86}Sr$ isotopic ratios of SCM, the elemental ratios of Lu/Hf and Rb/Sr can be estimated (Caro and Bourdon, 2010). These elemental constraints of the SCM can be summarized as (Caro and Bourdon, 2010):

$$(Sm/Nd)_{SCM} = 1.06(Sm/Nd)_{C\text{-}BSE}, \quad (1a)$$

$$(Lu/Hf)_{SCM} = 1.12(Lu/Hf)_{C\text{-}BSE}, \quad (1b)$$

$$(Rb/Sr)_{SCM} = 0.70(Rb/Sr)_{C\text{-}BSE}. \quad (1c)$$

All the currently available constraints for SCM come from these three isotopic systems and six elements, Sm, Nd, Lu, Hf, Rb, and Sr, and are summarized in Table 1. Uncertainties in the data are difficult to assess and not included because uncertainties in the ratios in various reservoirs are contentious. For example, Caro and Bourdon (2010) gave

Table 1
Inferred isotopic and elemental ratios for SCM compared to C-BSE.

	$\varepsilon^{142}Nd/^{144}Nd$	$^{143}Nd/^{144}Nd$	Sm/Nd	$^{176}Hf/^{177}Hf$	Lu/Hf	$^{87}Sr/^{86}Sr$	Rb/Sr
C-BSE	≡0	0.512634	0.3249	0.282786	0.2356	0.7050	0.03189
SCM	+0.18	0.51299	0.3446	0.283146	0.2641	0.7032	0.02245
Ratio			1.06		1.12		0.70

Elemental ratios Sm/Nd, Lu/Hf and Rb/Sr are given as mass ratios. The Sm/Nd ratio in SCM depends on the assumed timing of Sm/Nd differentiation. The last row (Ratio) is the normalized ratio of SCM to C-BSE. Some values are very slightly different from those listed in Caro and Bourdon (2010) because of re-evaluation and re-calculation in this work to maintain self consistency.

relatively small errors to these ratios, but Huang et al. (2013) argued that the $^{142}Nd/^{144}Nd$ ratio in chondrites is variable with total variation of about 50 ppm (i.e., ±0.50 epsilon units), meaning that all of the estimated ratios in SCM are within error the same as those in C-BSE. Jackson and Jellinek (2013) used these ratios at their face value to infer an SCM composition characterized by the low-$^4He/^3He$ mantle. The main goal of this work is not to settle the debate or to resolve the error bars, but to explore the consequence of the proposed superchondritic Earth using the ratios in Table 1 at their face values, and especially to evaluate whether this SCM can be related to C-BSE by removing a small fraction of partial melt and whether it is still appropriate to use C-BSE as normalization reference even if basalts are partial melting products of SCM. In order to use the constraints quantitatively, it is necessary to quantify the incompatibility sequence.

3. Comparison with the incompatibility sequence

The method adopted in this work is to compare the known constraints (known Sm/Nd, Lu/Hf and Rb/Sr ratios) for SCM with compositions of DMM to derive the systematics of SCM composition. The elements Sm, Nd, Lu, Hf, Rb, and Sr are all incompatible lithophile elements during mantle depletion and are variably depleted in DMM due to their different degrees of incompatibility. For rare earth elements, the lighter elements are more incompatible than the heavier elements (Gast, 1968). For other elements, the sequence of incompatibility has been evaluated empirically. For example, Sun and McDonough (1989) determined the following incompatibility sequence during mantle partial melting:

$$\begin{aligned}&\text{Cs}\approx\mathbf{Rb}\approx\text{Ba}>\text{Th}>\text{U}\approx\text{Nb}\approx\text{Ta}\approx\text{K}>\text{La}>\text{Ce}>\text{Pr}\approx\mathbf{Sr}>\mathbf{Nd}\approx\text{P}>\textit{Pm}>\\&\mathbf{Sm}\approx\text{Zr}\approx\mathbf{Hf}>\text{Eu}\approx\text{Ti}>\text{Gd}>\text{Tb}>\text{Dy}\approx\text{Li}>\text{Ho}\approx\text{Y}>\text{Er}>\text{Tm}>\text{Yb}>\mathbf{Lu},\end{aligned}\quad(2)$$

where the six elements of interest are noted in bold. The above list differs slightly from that of Sun and McDonough (1989) in (i) missing REE elements (including *Pm* with no stable isotope and Lu) are added to avoid "gaps" in the sequence; and (ii) some less characterized (volatile or siderophile or chalcophile) elements (such as Tl ≈ Rb; W ≈ Rb; Pb ≈ Ce; Mo ≈ Pr; F ≈ *Pm*; Sb ≈ Ti, and Sn ≈ Ti) are excluded, which did not produce any new gap in the elemental sequence. For clarity, only one element in the group of elements with nearly identical incompatibility is listed in the following sequence (except for Sm ≈ Hf, which are both included because they belong to the six elements of interest), and the six elements of interest are noted in bold:

$$\begin{aligned}&\mathbf{Rb}>\text{Th}>\text{U}>\text{La}>\text{Ce}>\mathbf{Sr}>\mathbf{Nd}>\textit{Pm}>\mathbf{Sm}\approx\mathbf{Hf}>\\&\text{Eu}>\text{Gd}>\text{Tb}>\text{Dy}>\text{Ho}>\text{Er}>\text{Tm}>\text{Yb}>\mathbf{Lu}.\end{aligned}\quad(3)$$

It can be noted that the six elements of interest cover the entire incompatibility sequence above. Because the parent element Sm (^{146}Sm and ^{147}Sm) is less incompatible than the daughter element Nd (^{142}Nd and ^{143}Nd), the parent element Lu is less incompatible than the daughter element Hf, but Rb is more incompatible than Sr, the enrichment of Sm/Nd and Lu/Hf ratios but the depletion of Rb/Sr ratio in SCM compared to C-BSE (Table 1) is qualitatively consistent with the mantle depletion process. That is, SCM is qualitatively consistently with a partially depleted C-BSE.

Next, it is necessary to quantify the incompatibility sequence because there is no reason to believe that spacing between two adjacent incompatible elements is constant. For example, Sm (the parent) is 2 elements behind Nd (the daughter) in the above incompatibility sequence, and Sm/Nd ratio in SCM is 6% enriched compared to C-BSE. Lu is 9 elements behind Hf in the sequence, Lu/Hf ratio in SCM is 12% enriched compared to C-BSE. On the other hand, Rb is 5 elements ahead of Sr in the sequence, and Rb/Sr ratio in SCM is 30% depleted compared to C-BSE. Hence, without quantification of the incompatibility, it is impossible to quantitatively relate the Sm/Nd, Lu/Hf, and Rb/Sr ratios to depletion, to examine whether SCM is related to DMM, and to derive the full SCM composition.

4. Quantification of the incompatibility sequence

To examine the incompatibility sequence quantitatively, two methods may be used. One is to use the partition coefficients of various elements between mantle rocks and mantle-derived melt. There is a huge literature on partition coefficients between mantle minerals and basaltic melts (e.g., review by Blundy and Wood, 2003; Geochemical Earth Reference Model website, http://earthref.org/GERM/). For mantle minerals, clinopyroxene is often the major reservoir for many trace elements. Hence, partition coefficients between clinopyroxene and basaltic melt have been investigated extensively. There is often significant scatter even for the partitioning of a given element between clinopyroxene and basaltic melt. For example, over 20 papers reported La partition coefficient between clinopyroxene and basalt (including alkali basalt) determined by studying phenocryst–matrix pairs or by experiments, and most values cluster in the range of 0.031 to 0.08, but some values can be up to 0.77 (Geochemical Earth Reference Model website, http://earthref.org/GERM/). Other mantle minerals include orthopyroxene, olivine, spinel and garnet. Kelemen et al. (2003), Donnelly et al. (2004) and Workman and Hart (2005) assessed and compiled mineral-melt and/or bulk partition coefficients of various elements. These three sets of estimated partition coefficients are shown in Fig. 1a using the elemental sequence above. Fig. 1a roughly confirms the incompatible elemental sequences of Sun and McDonough (1989) with more incompatible elements having smaller bulk partition coefficient. It can be see that the spacing between partition coefficients of neighboring elements is not equal (and nobody claimed that the spacing should be equal): between adjacent elements from Rb to Ce, the partition coefficients vary by a much larger factor than from Ce to Lu.

Another method to quantify the elemental incompatibility is to examine the depletion of the elements in DMM. This approach would work best for lithophile elements because atmophile elements can be additionally influenced by degassing, and siderophile and chalcophile elements (such as Pb) may be gradually sequestered by Earth's core. SS2004 and WH2005 estimated the composition of DMM by referencing to C-BSE of MS1995. SS2004 made elaborated effort to assess various elemental ratios in DMM using MORB samples and also made use of isotopic ratio constraints to estimate the concentration of each element in DMM (e.g., their Fig. 1 shows the genealogy of the approach). On the other hand, WH2005 compiled data on abyssal peridotites and derived inter-elemental relations in the mantle, and supplemented the data by isotopic ratio constraints and some canonical elemental ratios to derive DMM composition. Concentrations of incompatible elements in DMM normalized to those in C-BSE (MS1995) are plotted in Fig. 1b. Similar to Fig. 1a, there is general consistency in DMM composition and the incompatibility sequence, and the degrees of depletion of elements is not equally spaced for the elements in the incompatibility sequence. The shape of the curves in Fig. 1b is similar to that in Fig. 1a.

To determine the compositional relation between partially depleted mantles but at different degrees, model calculations are carried out for elements with different partition coefficients using repeated partial melting model (Hofmann, 1988). Fig. 2 shows how mantles depleted to different degrees are related, by plotting normalized concentrations of partially depleted mantle with between 3% and 15% partial melting, against a highly depleted mantle (15% partial melting) in a log–log plot, and the relations are linear. That is, when normalized concentrations of a less depleted mantle are plotted against those of DMM in a log–log plot, the trend should be linear if they can be traced back to a common primary mantle. Fig. 2 also shows how the melt composition (composition of a mantle-derived basalt) is related to mantle composition, and the relation is curved in log–log plot.

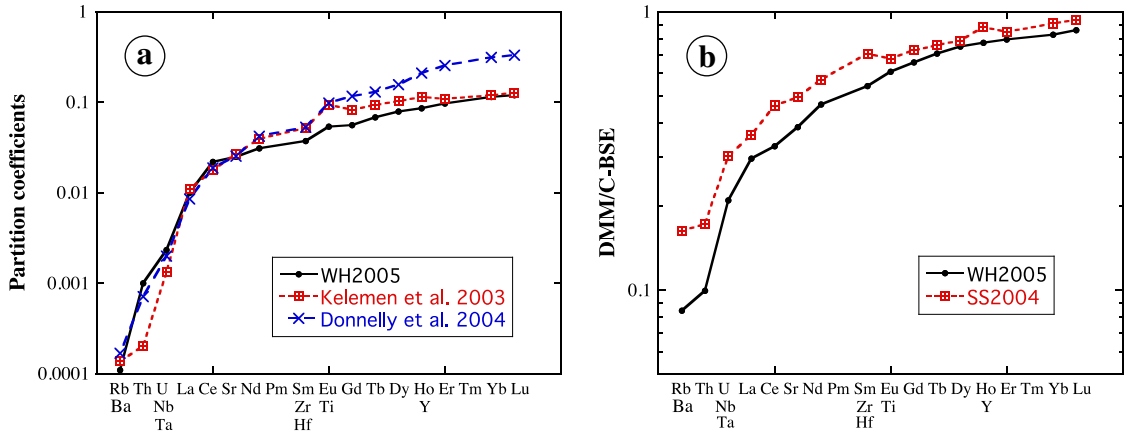

Fig. 1. (a) Partition coefficients between mantle and melt. The bulk partition coefficients of WH2005 are from their Table 2, those of Kelemen et al. (2003) are from their mineral–melt partition coefficients using a peridotite with 58% olivine, 20% opx, 20% cpx, and 2% spinel, and those of Donnelly et al. (2004) are from their mineral–melt partition coefficients using a peridotite with 60% olivine, 15% opx, 20% cpx, and 5% garnet. The proportions of minerals in spinel and garnet peridotites reflect mass balance of phase reactions. The bulk partition coefficient of Rb of WH2005 is revised to 0.00010 from their value 0.00001 so that Rb bulk partition coefficient is similar to that of Ba (0.00012) because Rb and Ba have similar incompatibility (e.g., Sun and McDonough, 1989, as well of Rb versus Ba concentration plot for MORB glasses in GeoRoc data). (b) Elemental concentrations in DMM normalized to those in C-BSE. C-BSE composition is from MS1995. DMM compositions are from SS2004 and WH2005. For elements with similar incompatibility, the values of partition coefficients and normalized concentrations are averaged (geometric average).

I propose to quantify the incompatibility sequence using the estimated DMM composition for lithophile elements. Define Compatibility Index (CoI) as follows:

$$\mathrm{CoI} = \ln(C_{\mathrm{DMM}}/C_{\mathrm{C\text{-}BSE}}), \tag{4}$$

where CoI is the compatibility index (not abbreviated as CI to avoid confusion with carbonaceous chondrite CI), and C_{DMM} and $C_{\mathrm{C\text{-}BSE}}$ are the concentrations of an element in DMM and in C-BSE. The logarithm scale is used so as to distinguish the highly incompatible elements, and to preserve the linear correlation when the normalized concentrations of partially depleted mantle in log scale is plotted against CoI. The index is called CoI (Compatibility Index) and not Incompatibility Index because the index is negative for incompatible elements, zero for a neutrally compatible (or neutrally incompatible) element, and positive for compatible elements, and CoI value decreases as the degree of incompatibility increases. Furthermore, more negative CoI values (for more incompatible elements) are plotted to the left following conventional spidergrams and the value increases from left to right on the horizontal axis. The incompatibility index may be defined as −CoI (negative CoI).

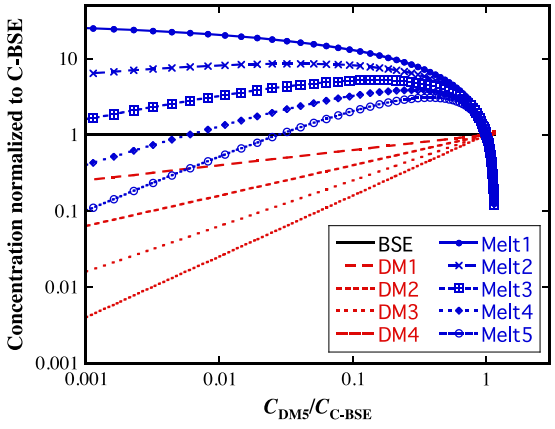

Fig. 2. Comparison of normalized concentrations between different partially depleted mantles and melts. All concentrations are normalized to the primitive mantle. DM1 is the residual mantle after removing 3% partial melt from primitive mantle using the batch-melting model. Melt 1 is the corresponding melt. DM2 is the residual mantle after 3% partial melting of DM1. DM3 is after 3% partial melting of DM2, and so forth.

Two papers reported systematically assessed DMM composition (SS2004; WH2005) and they are in general consistent with each other (Fig. 1b). Because DMM is heterogeneous with various degrees of depletion, the small difference between the trend of SS2005 and that of WH2005 in Fig. 1b can be interpreted to mean that SS2004 chose a less depleted member to represent DMM than WH2005. A more significant difference between SS2004 and WH2005 is that SS2004 reported concentrations of almost all elements, whereas WH2005 only reported concentrations of selected elements.

The CoI values of lithophile trace elements and major and minor elements are calculated from both DMM compositions and are listed in Table 2 (using DMM composition of SS2004) and Table 3 (using DMM composition of WH2005). The calculation does not include non-lithophile trace elements because concentrations of atmophile, siderophile, and chalcophile elements may be affected additionally by processes other than solid–melt partitioning (such as degassing and extraction to the core), and hence one single CoI value may not be enough to characterize the behavior of such elements. In Tables 2 and 3, three decimal places are retained for CoI values so that the calculation process does not introduce any new (truncation) errors even though the data precision is not high enough to warrant 3 decimal places in the CoI values.

Comparing CoI values based on DMM composition of SS2004, and those based on WH2005, for the same element, the absolute value of CoI based on SS2004 is smaller than that based on WH2005, as expected from Fig. 1b. After some comparison and evaluation, it is decided not to take a preference of the two different DMM compositions, and both are discussed below and will be distinguished as $\mathrm{CoI}_{\mathrm{WH2005}}$ and $\mathrm{CoI}_{\mathrm{SS2004}}$. One advantage of using $\mathrm{CoI}_{\mathrm{SS2004}}$ is that more elements were evaluated by SS2004 although there seems to be more scatter in plots using $\mathrm{CoI}_{\mathrm{SS2004}}$.

The relation between CoI values and partition coefficients is shown in Fig. 3. The partition coefficient on log scale is roughly linear with CoI values, but there is significant scatter for Th and U. Among the sets of bulk partition coefficients, best log–linear relation with CoI values is that of Kelemen et al. (2003) assuming 58% olivine, 20% orthopyroxene, 20% clinopyroxene, and 2% spinel. It may be argued that the CoI values are essentially linear to logK_{d} where K_{d} is partition coefficient. In the future, better constrained DMM composition and partition coefficients may be combined to carry out a total inversion to obtain a more accurate set of CoI values.

Below are some comments about CoI values listed in Tables 2 and 3: (1) In future applications, it is not necessary to plot elements with

Table 2
CoI of lithophile elements and concentration of lithophile elements in SCM based on the DMM composition of SS2004.

Elements	Conc in C-BSE	Conc in DMM	Normalized DMM	CoI_{SS2004}	Conc in SCM	Normalized SCM
Cs	0.021	0.00132	0.063	−2.767	0.0091	0.435
Rb	0.600	0.088	0.147	−1.920	0.337	0.561
Th	0.0795	0.0137	0.172	−1.758	0.0468	0.589
Ba	6.60	1.20	0.182	−1.705	3.95	0.599
B	0.30	0.060	0.200	−1.609	0.185	0.616
U	0.0203	0.0047	0.232	−1.463	0.0131	0.644
K	240	60	0.250	−1.386	158	0.659
Nb	0.658	0.21	0.319	−1.142	0.467	0.709
La	0.648	0.234	0.361	−1.019	0.477	0.736
Be	0.068	0.025	0.368	−1.001	0.0503	0.740
Ta	0.037	0.0138	0.373	−0.986	0.0275	0.743
Li	1.60	0.70	0.438	−0.827	1.25	0.780
F	25	11	0.440	−0.821	19.5	0.781
P	90	40.7	0.452	−0.796	70.9	0.788
Ce	1.675	0.772	0.461	−0.775	1.33	0.792
Sr	19.9	9.8	0.492	−0.708	16.1	0.808
Pr	0.254	0.131	0.516	−0.662	0.208	0.819
Nd	1.25	0.713	0.570	−0.561	1.06	0.845
Ti	1205	798	0.662	−0.412	1064	0.883
Sm	0.406	0.270	0.665	−0.408	0.359	0.884
Eu	0.154	0.107	0.665	−0.364	0.138	0.896
Hf	0.283	0.199	0.703	−0.352	0.255	0.899
Gd	0.544	0.395	0.726	−0.320	0.494	0.908
Zr	10.5	7.94	0.756	−0.279	9.65	0.919
Tb	0.099	0.075	0.758	−0.278	0.0911	0.920
Dy	0.674	0.531	0.788	−0.238	0.627	0.931
Na	2670	2151	0.806	−0.216	2502	0.937
Ho	0.149	0.122	0.819	−0.200	0.140	0.942
Er	0.438	0.371	0.847	−0.166	0.417	0.951
Tm	0.068	0.060	0.882	−0.125	0.0655	0.963
Yb	0.441	0.401	0.909	−0.095	0.429	0.972
Lu	0.0675	0.063	0.933	−0.069	0.066	0.979
Y	*4.3*	*4.07*	*0.946*	*−0.055*	*4.23*	*0.984*
Cr	*2625*	*2500*	*0.952*	*−0.049*	*2587*	*0.985*
V	82	79	0.963	−0.037	81.1	0.989
Mn	*1045*	*1045*	*1.000*	*0.000*	*1045*	*1.000*
Ni	*1960*	*1960*	*1.000*	*0.000*	*1960*	*1.000*
SiO_2 (wt.%)	45.00	44.90	0.998	−0.002	44.97	0.999
Al_2O_3 (wt.%)	4.45	4.28	0.962	−0.039	4.40	0.988
FeOt (wt.%)	8.05	8.07	1.002	0.002	8.06	1.001
MgO (wt.%)	37.80	38.22	1.011	0.011	37.93	1.003
CaO (wt.%)	3.55	3.50	0.986	−0.014	3.53	0.996
Na_2O (wt.%)	0.36	0.29	0.806	−0.216	0.337	0.937

C-BSE composition is from MS1995. Concentrations are in mass ppm unless otherwise indicated. Normalization is relative to C-BSE. Italics indicate inconsistency with empirical incompatibility sequence (e.g., Cr is likely a compatible element but its CoI value is negative using SS2004, whereas Mn and Sc are likely incompatible but CoI ≥ 1. Moreover, Ni is clearly more compatible than Fe and Mn but CoI values do not reflect that), and these values are not recommended to be used.

similar incompatibility at the same position in *x*-axis, because the CoI values carry the information quantitatively. (2) The CoI values for Nb and Ta are different ($\Delta CoI_{SS2004,Nb-Ta} = -0.156$; $\Delta CoI_{WH2005,Nb-Ta} = -0.140$, similar to the difference between Dy and Lu), so are those for Zr and Hf ($\Delta CoI_{SS2004,Zr-Hf} = +0.073$; $\Delta CoI_{WH2005,Zr-Hf} = -0.137$), suggesting that the notion that each pair of Zr–Hf and Nb–Ta have essentially identical properties is not correct, as pointed out by previous authors (Niu and Batiza, 1997; Salters and Longhi, 1999; Salters et al., 2002; Münker et al., 2003; Niu, 2004, 2012; Pfander et al., 2007). Nonetheless, the differences are within uncertainties of elemental concentration estimates by MS1995, SS2004 and WH2005.

One application of the CoI values is to be used as horizontal axis in spidergrams. Fig. 4 shows spidergrams of DMM and MORB using CoI. Fig. 4a uses CoI_{WH2005} as the horizontal axis, and Fig. 4b uses CoI_{SS2004} as the horizontal axis. From Fig. 4a, DMM composition trend of SS2004 when plotted against CoI values based on WH2005 is almost linear with less depletion, but there are also some small spikes indicating small inconsistency between the two estimates. The trends for MORB show weak nonlinearity toward the less incompatible elements (as CoI approaching zero), consistent with Fig. 2. On the other hand, if CoI_{SS2004} is used (Fig. 4b), many more elements can be plotted, but there are larger spikes (for elements Ba, Be, Li, F, and Cr, etc.), indicating inconsistency among different estimates on these elements. There are at least two advantages for using CoI values in spidergrams. One is that the horizontal axis is quantified rather than equally spaced elements. Hence, elements with similar incompatibility or different incompatibility can be handled consistently and in theory more accurately when using CoI values than arranging elements in an array with equal spacing in traditional spidergrams. Secondly, normalized concentrations in log scale for mantle samples depleted to various degrees are linear with CoI values (Fig. 4), rather than curved as in Fig. 1b. It is easier to map out departure (or anomalies) from a linear trend than from a curved trend to discuss possible enrichment and depletion of elements due to fluid involvement or residual phases.

The CoI values developed above are best applied to study mantle samples. For basalt samples, there are some disadvantages of using these CoI values. One is that the trend for normalized concentrations is curved (Figs. 2 and 4). Second and more importantly, the CoI values do not distinguish slightly incompatible and especially compatible elements well. For example, CoI values for V, Sc, and Cr are all clustered at about 1. This is because DMM is produced by only small degrees of depletion and hence the concentrations of compatible elements have not changed much. To derive a set of CoI values better applicable to basalts, one may start from partition coefficients, or from assessed mean composition of basalts from C-BSE or SCM, such as Hawaii basalts. It may also be necessary to consider the variation of melt composition

Table 3
CoI of lithophile elements and concentration of lithophile elements in SCM based on the DMM composition of WH2005.

Element	Conc in C-BSE	Conc in DMM	Normalized DMM	CoI_{WH2005}	Conc in SCM	Normalized SCM
Rb	0.6	0.05	0.083	−2.485	0.335	0.558
Ba	6.6	0.563	0.085	−2.462	3.70	0.561
Th	0.0795	0.0079	0.099	−2.309	0.0462	0.581
U	0.0203	0.00317	0.156	−1.847	0.0132	0.648
K	240	50	0.208	−1.569	166	0.692
Nb	0.658	0.1485	0.226	−1.489	0.464	0.705
Ta	0.037	0.0096	0.259	−1.349	0.0269	0.728
La	0.648	0.192	0.296	−1.216	0.487	0.751
Ce	1.675	0.55	0.328	−1.114	1.29	0.770
Sr	19.9	7.664	0.385	−0.954	15.9	0.799
Pr	0.254	0.107	0.421	−0.865	0.207	0.816
Nd	1.25	0.581	0.465	−0.755	1.044	0.835
Zr	10.5	5.082	0.484	−0.726	8.85	0.843
Hf	0.283	0.157	0.555	−0.589	0.246	0.871
Sm	0.406	0.239	0.589	−0.530	0.358	0.883
Ti	1205	716.3	0.594	−0.520	1066	0.885
Eu	0.154	0.096	0.623	−0.473	0.138	0.895
Gd	0.544	0.358	0.658	−0.418	0.493	0.906
Tb	0.099	0.0697	0.704	−0.347	0.0913	0.922
Dy	0.674	0.505	0.749	−0.289	0.630	0.934
Ho	0.149	0.115	0.772	−0.259	0.140	0.941
Y	4.3	3.328	0.774	−0.256	4.05	0.942
Er	0.438	0.348	0.795	−0.230	0.415	0.947
Yb	0.441	0.365	0.828	−0.189	0.422	0.957
Lu	0.0675	0.058	0.859	−0.152	0.0651	0.965
P_2O_5 (wt.%)	*0.0210*	*0.0190*	*0.905*	*−0.100*	*0.0205*	*0.977*
NiO (wt.%)	*0.250*	*0.240*	*0.960*	*−0.041*	*0.248*	*0.990*
MnO (wt.%)	*0.135*	*0.130*	*0.963*	*−0.038*	*0.134*	*0.991*
Cr_2O_3 (wt.%)	*0.384*	*0.570*	*1.484*	*0.395*	*0.421*	*1.097*
SiO_2 (wt.%)	45.00	44.71	0.994	−0.006	44.93	0.998
Al_2O_3 (wt.%)	4.45	3.98	0.894	−0.112	4.33	0.974
FeOt (wt.%)	8.05	8.18	1.016	0.016	8.08	1.004
MgO (wt.%)	37.80	38.73	1.025	0.024	38.02	1.006
CaO (wt.%)	3.55	3.17	0.893	−0.113	3.46	0.974
Na_2O (wt.%)	0.36	0.28*	0.778	−0.251	0.34	0.943

C-BSE composition is from MS1995. Concentrations are in mass ppm unless otherwise indicated. Normalization is relative to C-BSE. Italics indicate inconsistency with empirical incompatibility sequence (e.g., P is likely more incompatible than indicated here, and Ni is compatible but is not shown by the CoI value), and these values are not suggested to be used.
* WH2005 gave two values for Na_2O, and one is chosen here.

with not only the degree of partial melting, but also the depth of partial melting (e.g., SiO_2 can range from slightly incompatible to slightly compatible when the depth of partial melting increases).

5. Superchondritic mantle is partially depleted chondritic mantle

The quantified CoI values can now be compared with the constraints for SCM. For SCM, the constraints are on Sm/Nd, Lu/Hf, and Rb/Sr elemental ratios, rather than elemental concentrations. Hence, it is necessary to make normalized ratio plot rather than normalized concentration plot. Because (using Sm/Nd as an example)

$$\ln\left[(Sm/Nd)_{SCM}/(Sm/Nd)_{C\text{-}BSE}\right] = \ln(Sm_{SCM}/Sm_{C\text{-}BSE}) - \ln(Nd_{SCM}/Nd_{C\text{-}BSE}), \quad (5a)$$

$$\ln\left[(Sm/Nd)_{DMM}/(Sm/Nd)_{C\text{-}BSE}\right] = CoI_{Sm} - CoI_{Nd} = \Delta CoI, \quad (5b)$$

the comparison is made as:

$$\ln[ratio_{SCM}/ratio_{C\text{-}BSE}] \text{ versus } \Delta CoI, \quad (6)$$

where ratio means the parent/daughter ratio, and ΔCoI means the difference in CoI value of parent nuclide (element) minus that of the daughter nuclide (element). In such a plot, a linear relation between the logarithm of normalized ratios in SCM and ΔCoI passing through the origin (0,0) can be interpreted as SCM and DMM being related to the same C-BSE by different degrees of partial melting, similar to the linear trend of DM1 (and DM2, DM3, DM4) relative to DM5 in log scale passing through point (1,1) in Fig. 2.

Fig. 5 compares the depletion or enrichment of parent/daughter ratios in SCM with ΔCoI (that is, depletion or enrichment in DMM). The data lie almost perfectly on a straight line passing through (0,0). The best-fit equations are as follows:

$$\ln(ratio_{SCM}/ratio_{C\text{-}BSE}) = 0.235 \times \Delta CoI_{WH2005} = 0.235 \times \ln\left(ratio_{DMM_{WH2005}}/ratio_{C\text{-}BSE}\right), \quad (7a)$$

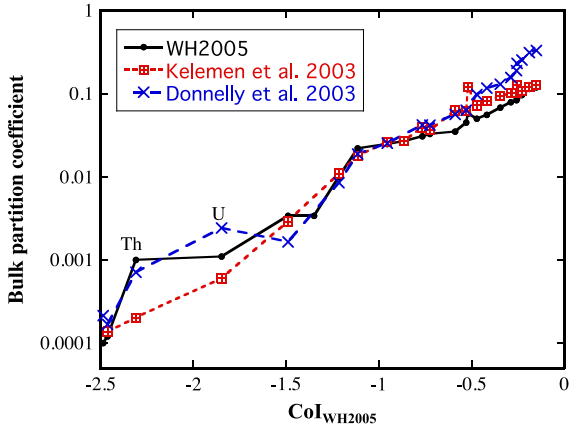

Fig. 3. The relation between CoI values and bulk partition coefficients between mantle materials and basaltic melt.

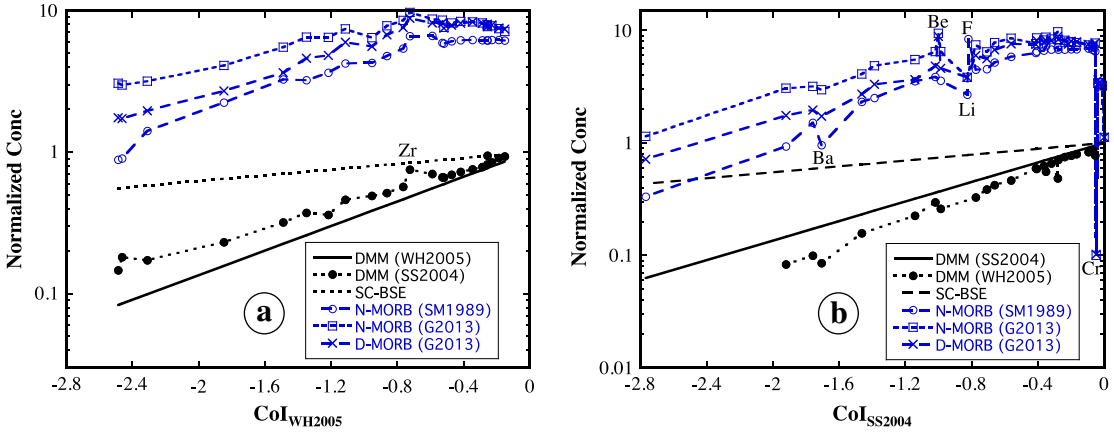

Fig. 4. Spidergrams of DMM (SS2004; WH2005) and average N-type MORB (Sun and McDonough, 1989; Gale et al., 2013) and depleted MORB (D-MORB) (Gale et al., 2013) using CoI values based on (a) WH2005 or (b) SS2004 as the horizontal axis.

$$\ln(\text{ratio}_{SCM}/\text{ratio}_{C\text{-}BSE}) = 0.301 \times \Delta\text{CoI}_{SS2004} = 0.301 \times \ln\left(\text{ratio}_{DMM_{SS2004}}/\text{ratio}_{C\text{-}BSE}\right). \quad (7b)$$

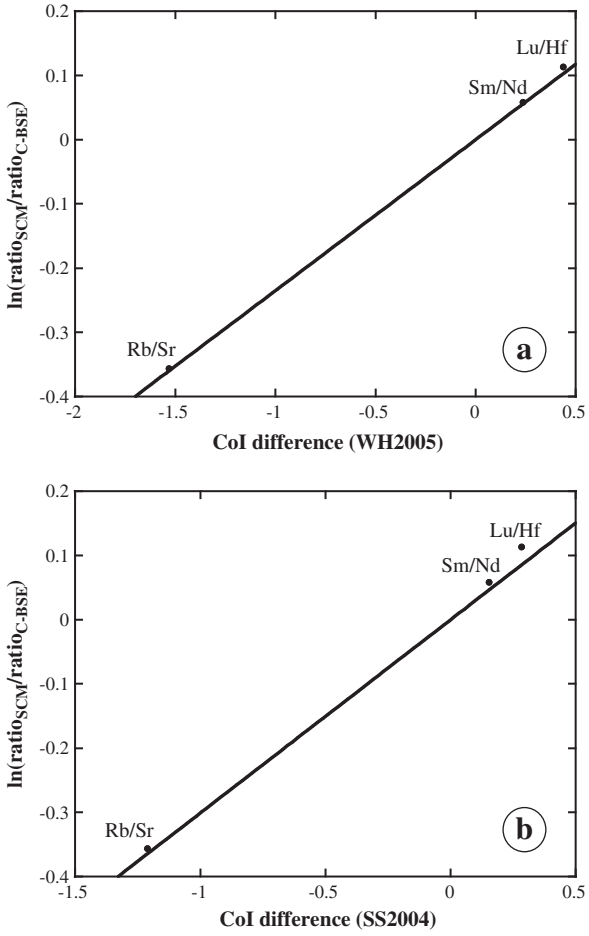

Fig. 5. Comparison between SCM and DMM for Sm/Nd, Lu/Hf, and Rb/Sr ratios. The horizontal axis is $\text{CoI}_{parent} - \text{CoI}_{daughter}$, which is equivalent to $\ln(\text{ratio}_{DMM} / \text{ratio}_{C\text{-}BSE})$. The data are fit by a straight line passing through the origin, meaning only the slope is fit. (a) Using CoI values of WH2005. The slope of the best-fit line is 0.235 ± 0.005 (correlation coefficient $r = 0.9995$). (b) Using CoI values of SS2004. The slope is 0.301 ± 0.018 (correlation coefficient $r = 9962$).

Therefore, it can be argued that both SCM and DMM are derived from the same C-BSE but with different degrees of depletion. Assuming the above equations hold for all arbitrary lithophile elemental ratios, the following can be derived:

$$\ln(C_{SCM}/C_{C\text{-}BSE}) \approx 0.235 \times \ln\left(C_{DMM_{WH}2005}/C_{C\text{-}BSE}\right), \quad (8a)$$

$$\ln(C_{SCM}/C_{C\text{-}BSE}) \approx 0.301 \times \ln\left(C_{DMM_{SS}2004}/C_{C\text{-}BSE}\right). \quad (8b)$$

Hence, the composition of SCM can be derived (see next section).

Because the relations in Fig. 5 suggests that the processes for making SCM from C-BSE is similar to those for making DMM from C-BSE, compositionally, superchondritic mantle can be interpreted to be partially depleted chondritic mantle, with degree of depletion about a quarter of the way (0.235 to 0.301) compared to the present-day depleted MORB mantle. Because different planets unlikely have the same differentiation trends in terms of Sm/Nd, Lu/Hf and Rb/Sr (note that Rb is not a refractory element), the easiest explanation is that Earth started with chondritic refractory elemental composition, consistent with observed $^{142}Nd/^{144}Nd$ anomalies being either nucleosynthetic or due to internal Earth evolution, such as the hidden reservoir model of Boyet and Carlson (2005), or the impact erosion model of O'Neill and Palme (2008) and Campbell and O'Neill (2012). Whether the subchondritic reservoir is hidden or lost by impact has important implications on Earth's heat budget and thermal evolution and can be resolved decisively by more precise geoneutrino measurements (Dye, 2012). Current geoneutrino data are consistent with Th and U concentrations at the C-BSE level but cannot rule out other possibilities (e.g., Gaodo et al., 2011).

Using the interpretation that the superchondritic mantle is partially depleted chondritic mantle, the composition of the "primitive" superchondritic mantle (SCM) is derived below.

6. Composition of the superchondritic mantle

Knowing the relation between SCM to DMM, the composition of primitive SCM can be estimated using either Eqs. (8a) or (8b). The concentrations of the elements in SCM thus calculated are shown in the last 2 columns of Table 2 based on DMM of SS2004 and Table 3 based on DMM of WH2005. The normalized compositions of SCM are shown in Fig. 4 as dashed lines. Even though the DMM composition of SS2004 is systematically different from that of WH2005 (Fig. 1b), because the SCM composition is obtained by anchoring to the same constraints (Table 1), it is expected that the SCM composition obtained from DMM of SS2004 is similar to that from DMM of WH2005. Fig. 6a compares normalized elemental concentrations in SCM using two different

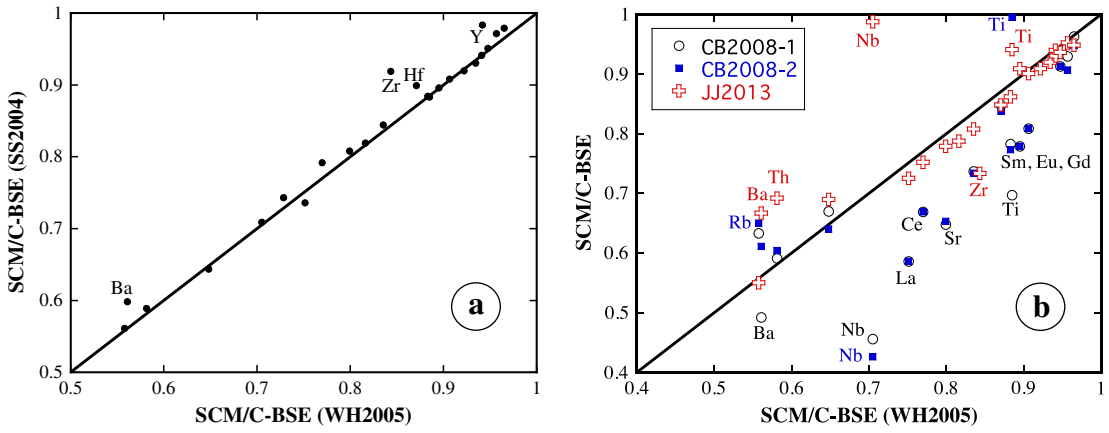

Fig. 6. (a) Comparison of the SCM composition obtained in this study using DMM of SS2004 and of WH2005. (b) Comparison of the SCM (or early depleted reservoir EDR) composition obtained by Carlson and Boyet (2008) and Jackson and Jellinek (2013) with that of DMM WH2005 (this work). Carlson and Boyet (2008) listed two EDR compositions in their Table 1 and they are both shown here as CB2008-1 and CB2008-2. The concentrations are normalized to C-BSE. The solid line is 1:1 line.

DMM compositions. Except for Zr (9% relative difference), Ba (7% relative difference), and Y (4% relative difference), all other elements compare very well within a few percent. That is, the concentrations of lithophile elements in SCM are well constrained no matter whose DMM composition is used.

Because the issue whether or not there is a hidden subchondritic reservoir is not resolved, the consequences of the SCM in terms of Ar budget and volume of undegassed mantle (e.g., Zhang and Zindler, 1989; Allegre et al., 1996; Zhang, 1998, 2002; Jackson and Jellinek, 2013), compositional rebalance between crust and mantle (e.g., Caro and Bourdon, 2010), and heat budget and thermal evolution of Earth (e.g., O'Neill and Palme, 2008) are not discussed. My preference is that subchondritic materials are hidden in Earth (D″ layer and the unsampled lower crust), meaning that SCM is not the same as BSE, and hence the derived SCM composition does not lead to new global consequences.

7. Comparison with previous work

This work draws heavily from the work of Caro and Bourdon (2010) on Sm/Nd, Lu/Hf, and Rb/Sr ratios in SCM, which are used to demonstrate the relation between SCM and DMM. This work focuses on (i) developing the method to infer the composition of SCM, (ii) showing that SCM composition is related to DMM composition, and (iii) providing the composition of SCM, whereas Caro and Bourdon (2010) explored consequences of the superchondritic composition on mantle–crust evolution.

O'Neill and Palme (2008) proposed that collisional erosion of protocrust and residual mantle was responsible for the superchondritic signature of the earth. There is some similarity between this work and their work, but also major differences. They started by arguing that the bulk earth has a superchondritic Fe/Mg ratio (2.11 in the bulk earth versus 1.92 ± 0.08 in chondrites). They further used the condition of superchondritic Sm/Nd and the assumption that K in SCM is about 50% (this work gives 66% to 69%, Tables 2 and 3) of that in C-BSE. With these three conditions, they constrained their collisional erosion model in which some proto-crust (equivalent to 0.014 times the mass of the final Earth) and residual mantle (equivalent to 0.086 times the mass of the final Earth) were lost to outer space (including the moon). They assumed but didn't demonstrate that the compositional constraints of the SCM are consistent with it being a partially depleted mantle. There are some difficulties with their model. First, considering that the present oceanic crust (60% of Earth's surface, 7 km average thickness, 2900 kg/m^3 density) is only about 0.10% of Earth mass and continental crust (40% of Earth's surface, 40 km average thickness, 2700 kg/m^3 density) only 0.37% of Earth mass, losing a protocrust equivalent to 1.4% Earth mass (equivalent to 14 current oceanic crusts) at the beginning of Earth history is not trivial (although not impossible) because it took time to produce such crusts repeatedly to be lost and because deep melting does not contribute to crustal growth (Stolper et al., 1981; Agee and Walker, 1988). On the other hand, hiding this mass in D″ layer (about 2.2% of Earth mass, Dziewonski and Anderson, 1981) and partially in the lower continental crust is possible and much easier. Second, the model of O'Neill and Palme (2008) was anchored by a K concentration in SCM to be 50% of that in C-BSE as an independent constraint of their model, which was considered by Jackson and Jellinek (2013) "to be more fraught with error" compared to other approaches. For example, my results show that K concentration in SCM is 66–69% of that in BSE.

Carlson and Boyet (2008) made effort to estimate the composition of the early depleted reservoir (EDR, equivalent to SCM in this study) using mass balance, C-BSE composition of MS1995, continental crust compositions of Taylor and McLennan (1985) and Rudnick and Gao (2003), and DMM composition of their own work (Boyet and Carlson, 2006). Jackson and Jellinek (2013), whose paper was published as this work was written up (Zhang, 2013), evaluated the composition of the low-^{4}He/^{3}He mantle (equivalent to SCM in this study) using the same Sm/Nd, Rb/Sr, and Lu/Hf ratio constraints as in this study, plus REE patterns of 18 selected peridotites thought to represent the low-^{4}He/^{3}He mantle, some elemental ratios, and Lu concentration anchored to 0.064 ppm. Their results are compared with this work in Fig. 6b. Though the approaches are different, it can be seen that the trends in Carlson and Boyet (2008) and Jackson and Jellinek (2013) are generally concordant with results in this work, and the more recent work by Jackson and Jellinek (2013) is more similar to this work, demonstrating rough consistency in various geochemical approaches. The most significant difference is in Nb concentration, probably due to low precision in estimated Nb concentration in continental crust used by Carlson and Boyet (2008), and inconsistencies when various ratios were constrained in the work of Jackson and Jellinek (2013).

Although there are similarities among the various papers, my approach differs from and complements the above papers. I quantify the elemental compatibility sequence and show that the known constraints of SCM are quantitatively consistent with SCM being a partially depleted C-BSE (Fig. 5), which were not attempted by earlier workers. The complete composition of lithophile elements in SCM is derived in a self-consistent way.

8. Summary and conclusions

In this work, the elemental incompatibility sequence used in spidergrams is quantified, and each element is assigned a "Compatibility Index" CoI. For incompatible elements, CoI is negative. Two sets of CoI

values are derived, one based on the DMM composition estimate of WH2005 (Table 3), and the other based on that of SS2004 (Table 2). Using CoI values as the horizontal axis and normalized concentrations as the vertical axis, the new spidergram for various mantle samples with different degree of depletion is roughly linear, but mantle-derived basalt samples are slightly curved for the less incompatible elements (Fig. 4), as expected (Fig. 2). It is expected that the quantification of CoI values will be improved in the future with better-constrained composition of the depleted MORB mantle and partition coefficients.

The constrained Sm/Nd, Lu/Hf and Rb/Sr ratios of the primitive superchondritic mantle (Caro and Bourdon, 2010) are shown to be quantitatively consistent with a partially depleted "chondritic" mantle. Because the six elements from which the SCM composition is constrained include not only refractory lithophile elements of Sr, Nd, Sm, Lu, and Hf, but also the volatile lithophile element of Rb, and because different planetary bodies rarely have similar Rb/Sr ratios, the easiest explanation is that the superchondritic mantle is partially depleted terrestrial mantle in the very early stage of mantle depletion and evolution, meaning subchondritic material is hidden somewhere such as D″ layer (Boyet and Carlson, 2005) and unsampled lower crust but may also be lost due to impacts (O'Neill and Palme, 2008). It is hoped that future geoneutrino measurements will resolve definitively whether Earth has chondritic Th and U concentrations. The very rapid early depletion is consistent with previous studies (e.g., Staudacher and Allegre, 1982; Hamilton et al., 1983; Albarede and Brouxel, 1987; Zhang and Zindler, 1989; Zhang, 2014), although precise quantification of timing and depletion degree is not available currently due to large error bars in the excess $^{142}Nd/^{144}Nd$ and Sm/Nd in Earth compared to chondrites. The lithophile elemental concentrations of the assumed superchondritic mantle (SCM) are derived with high precision (last two columns of Tables 2 and 3).

Because SCM is related to C-BSE by partial mantle depletion similar to that happened in the terrestrial mantle, when studying chemical compositions of basalt and other rocks using spidergrams, it is still appropriate to normalize elemental concentrations to C-BSE. Furthermore, the horizontal axis is now quantified using the Compatibility Index CoI.

Acknowledgements

I thank Shichun Huang and Vincent Salters for informal comments, and K. Mezger, H. Palme and an anonymous reviewer for insightful and constructive reviews. Financial support by NASA (NNX10AH74G) and NSF (EAR-1019440) is gratefully acknowledged.

References

Agee, C.B., Walker, D., 1988. Static compression and olivine flotation in ultrabasic silicate liquid. J. Geophys. Res. 93, 3437–3449.
Albarede, F., Brouxel, M., 1987. The Sm/Nd secular evolution of the continental crust and the depleted mantle. Earth Planet. Sci. Lett. 82, 25–35.
Allegre, C.J., Poirier, J.-P., Humler, E., Hofmann, A.W., 1995. The chemical composition of the earth. Earth Planet. Sci. Lett. 134, 515–526.
Allegre, C., Hofmann, A., O'Nions, R.K., 1996. The argon constraints on mantle structure. Geophys. Res. Lett. 23, 3555–3557.
Andreasen, R., Sharma, M., 2006. Solar nebula heterogeneity in p-process samarium and neodymium isotopes. Science 314, 806–809.
Blichert-Toft, J., Albarede, F., 1997. The Lu–Hf isotope geochemistry of chondrites and the evolution of the mantle–crust system. Earth Planet. Sci. Lett. 148, 243–258.
Blundy, J.D., Wood, B.J., 2003. Partitioning of trace elements between crystals and melts. Earth Planet. Sci. Lett. 210, 383–397.
Boyet, M., Carlson, R.W., 2005. ^{142}Nd evidence for early (>4.53 Ga) global differentiation of the silicate Earth. Science 309, 576–581.
Boyet, M., Carlson, R.W., 2006. A new geochemical model for the Earth's mantle inferred from ^{146}Sm–^{142}Nd systematics. Earth Planet. Sci. Lett. 250, 254–268.
Boyet, M., Blichert-Toft, J., Rosing, M., Storey, M., Telouk, P., Albarede, F., 2003. ^{142}Nd evidence for early Earth differentiation. Earth Planet. Sci. Lett. 214, 427–442.
Campbell, I.H., O'Neill, H.S.C., 2012. Evidence against a chondritic Earth. Nature 483, 553–558.
Carlson, R.W., Boyet, M., 2008. Composition of the Earth's interior: the importance of early events. Phil. Trans. R. Soc. A 366, 4077–4103.
Caro, G., Bourdon, B., Birck, J.-L., Moorbath, S., 2006. High-precision 142Nd/144Nd measurements in terrestrial rocks: constraints on the early differentiation of the Earth's mantle. Geochim. Cosmochim. Acta 70, 164–191.
Carlson, R.W., Boyet, M., Horan, M., 2007. Chondrite barium, neodymium, and samarium isotopic heterogeneity and early Earth differentiation. Science 316, 1175–1178.
Caro, G., Bourdon, B., 2010. Non-chondritic Sm/Nd ratio in the terrestrial planets: consequences for the geochemical evolution of the mantle–crust system. Geochim. Cosmochim. Acta 74, 3333–3349.
Caro, G., Bourdon, B., Birck, J.L., Moorbath, S., 2003. ^{146}Sm–^{142}Nd evidence from Isua metamorphosed sediments for early differentiation of the Earth's crust. Nature 423, 428–432.
Caro, G., Bourdon, B., Halliday, A.N., Qiuitte, G., 2008. Super-chondritic Sm/Nd ratios in Mars, the Earth and the Moon. Nature 450, 336–339.
Donnelly, K.E., Goldstein, S.L., Langmuir, C.H., Spiegelman, M., 2004. Origin of enriched ocean ridge basalts and implications for mantle dynamics. Earth Planet. Sci. Lett. 226, 347–366.
Dye, S.T., 2012. Geoneutrinos and the radioactive power of the earth. Rev. Geophys. 50, RG3007.
Dziewonski, A.M., Anderson, D.L., 1981. Preliminary reference Earth model. Phys. Earth Planet. Inter. 25, 297–356.
Fitoussi, C., Bourdon, B., 2012. Silicon isotope evidence against an enstatite chondrite Earth. Science 335, 1477–1480.
Gale, A., Dalton, C.A., Langmuir, C.H., Su, Y., Schilling, J.G., 2013. The mean composition of ocean ridge basalts. Geochem. Geophys. Geosyst. 14. http://dx.doi.org/10.1029/2012GC004334.
Gannoun, A., Boyet, M., Rizo, H., El Goresy, A., 2011. ^{146}Sm–^{142}Nd systematics measured in enstatite chondrites reveals a heterogeneous distribution of ^{142}Nd in the solar nebula. PNAS 108, 7693–7697.
Gaodo, A., Gaodo, Y., Ichimura, K., Ikeda, H., Inoue, K., Kibe, Y., Kishimoto, Y., Koga, M., et al., 2011. Partial radiogenic heat model for Earth revealed by geoneutrino measurements. Nat. Geosci. 4, 647–651.
Gast, P.W., 1968. Trace element fractionation and the origin of tholeiitic and alkaline magma types. Geochim. Cosmochim. Acta 32, 1057–1086.
Hamilton, P.J., O'Nions, R.K., Bridgewater, D., Nutman, A., 1983. Sm-Nd studies of Archean metasediments and metavolcanics from West Greenland and their implications for the Earth's early history. Earth Planet. Sci. Lett. 62, 263–272.
Harper, C.L., Jacobsen, S.B., 1992. Evidence from coupled ^{147}Sm–^{143}Nd and ^{146}Sm–^{142}Nd systematics for very early (4.5 Gyr) differentiation of the Earth's mantle. Nature 360, 728–732.
Hart, S.R., 1992. Mantle plumes and entrainment: isotopic evidence. Science 256, 517–520.
Hofmann, A.W., 1988. Chemical differentiation of the Earth: the relationship between mantle, continental crust, and oceanic crust. Earth Planet. Sci. Lett. 90, 297–314.
Huang, S., Jacobsen, S.B., Mukhopadhyay, S., 2013. ^{147}Sm–^{143}Nd systematics of Earth are inconsistent with a superchondritic Sm/Nd ratio. PNAS 110, 4929–4934.
Jackson, M.G., Carlson, R.W., 2012. Homogeneous superchondritic $^{142}Nd/^{144}Nd$ in the mid-ocean ridge basalt and ocean island basalt mantle. Geochem. Geophys. Geosyst. 13, Q06011 (06010.01029/02012GC004114).
Jackson, M.G., Jellinek, A.M., 2013. Major and trace element composition of high $^{3}He/^{4}He$ mantle: implications for the composition of a nonchondritic Earth. Geochem. Geophys. Geosyst. 14. http://dx.doi.org/10.1002/ggge.20188.
Jackson, M.G., Kurz, M.D., Hart, S.R., Workman, R.K., 2007. New Samoan lavas from Ofu Island reveal a hemispherically heterogeneous high $^{3}He/^{4}He$ mantle. Earth Planet. Sci. Lett. 264, 360–374.
Jagoutz, E., Palme, H., Baddenhausen, H., Blum, K., Cendales, M., Dreibus, G., Spettel, B., Lorenz, V., Wanke, H., 1979. The abundances of major, minor and trace elements in the earth's mantle as derived from primitive ultramafic nodules. Proc. Lunar Planet. Conf. 10, 2031–2050.
Javoy, M., 1995. The integral enstatite chondrite model of the earth. Geophys. Res. Lett. 22, 2219–2222.
Javoy, M., et al., 2010. The chemical composition of the Earth: enstatite chondrite models. Earth Planet. Sci. Lett. 293, 259–268.
Kelemen, P.B., Yogodzinski, G.M., Scholl, D.W., 2003. Along-strike variation in the Aleutian Island Arc: genesis of high-Mg# andesite and implications for continental crust. In: Eiler, J.M. (Ed.), Inside the Subduction Factory. AGU Monograph, Washington, DC, pp. 223–276.
Kinoshita, N., Paul, M., Kashiv, Y., Collon, P., Deibel, C.M., FDiGiovine, B., Greene, J.P., Henderson, D.J., Jiang, C.L., Marley, S.T., Nakanishi, T., Pardo, R.C., Rehm, K.E., Roberstson, D., Scott, R., Schmitt, C., Tang, X.D., Vondrasek, R., Yokoyama, A., 2012. A shorter ^{146}Sm half-life measured and implications for ^{146}Sm–^{142}Nd chronology in the solar system. Science 335, 1614–1617.
Lyubetskaya, T., Korenaga, J., 2007. Chemical composition of Earth's primitive mantle and its variance. J. Geophys. Res. 112, B03211. http://dx.doi.org/10.1029/2005JB004223.
McDonough, W.F., Sun, S.-S., 1995. The composition of the Earth. Chem. Geol. 120, 223–253.
Münker, C., Pfander, J.A., Weyer, S., Buchl, A., Kleine, T., Mezger, K., 2003. Evolution of planetary cores and the Earth–Moon system from Nb/Ta systematics. Science 301, 84–87.
Niu, Y., 2004. Bulk-rock major and trace element compositions of abyssal peridotites: implications for mantle melting, melt extraction and post-melting processes beneath mid-ocean ridges. J. Petrol. 45, 2433–2458.
Niu, Y., 2012. Earth processes cause Zr–Hf and Nb–Ta fractionations, but why and how? RSC Adv. 2, 3587–3591.
Niu, Y., Batiza, R., 1997. Trace element evidence from seamounts for recycled oceanic crust in the Eastern Pacific mantle. Earth Planet. Sci. Lett. 148, 471–483.

O'Neill, H.S.C., Palme, H., 2008. Collisional erosion and the non-chondritic composition of the terrestrial planets. Phil. Trans. R. Soc. A 366, 4205–4238.
Palme, H., O'Neill, H.S.C., 2004. Cosmochemical estimates of mantle composition. In: Holland, H.D., Turrekian, K.K. (Eds.), Treatise on Geochemistry. Elsevier, Amsterdam, pp. 1–38.
Pfander, J.A., Munker, C., Stracke, A., Mezger, K., 2007. Nb/Ta and Zr/Hf in ocean island basalts — implications for crust–mantle differentiation and the fate of niobium. Earth Planet. Sci. Lett. 254, 158–172.
Rubie, D.C., et al., 2011. Heterogeneous accretion, composition and core–mantle differentiation of the Earth. Earth Planet. Sci. Lett. 301, 31–42.
Rudnick, R.L., Gao, S., 2003. Composition of the continental crust. Treatise on Geochem 3, 1–64.
Salters, V.J., Longhi, J., 1999. Trace element partitioning during the initial stages of melting beneath mid-ocean ridges. Earth Planet. Sci. Lett. 166, 15–30.
Salters, V.J., Stracke, A., 2004. Composition of the depleted mantle. Geochem. Geophys. Geosyst. 5, Q05004.
Salters, V.J., Longhi, J.E., Bizimis, M., 2002. Near mantle solidus trace element partitioning at pressures up to 3.4 GPa. Geochem. Geophys. Geosyst. 3. http://dx.doi.org/10.1029/2001GC000148.
Staudacher, T., Allegre, C.J., 1982. Terrestrial xenology. Earth Planet. Sci. Lett. 60, 389–406.
Stolper, E., Walker, D., Hager, B.H., Hays, J.F., 1981. Melt segregation from partially molten source regions: the importance of melt density and source region size. J. Geophys. Res. 86, 6261–6271.
Sun, S.-S., 1982. Chemical composition and origin of the earth's primitive mantle. Geochim. Cosmochim. Acta 46, 179–192.
Sun, S., McDonough, W.F., 1989. Chemical and isotopic systematics of oceanic basalts: implications for mantle composition and processes. In: Sauders, A.D., Norry, M.J. (Eds.), Magmatism in the Ocean Basins. Geological Society Special Publication, pp. 313–345.
Taylor, S.R., McLennan, S.M., 1985. The Continental Crust: Its Composition and Evolution. Blackwell Scientific, Oxford, UK (311 pp.).
Vervoort, J.D., Patchet, P.J., Blichert-Toft, J., Albarede, F., 1999. Relationships between Lu–Hf and Sm–Nd isotopic systems in the global sedimentary system. Earth Planet. Sci. Lett. 168, 79–99.
Workman, R.K., Hart, S.R., 2005. Major and trace element composition of the depleted MORB mantle (DMM). Earth Planet. Sci. Lett. 231, 53–72.
Zambardi, T., et al., 2013. Silicon isotope variations in the inner solar system: implications for planetary formation, differentiation and composition. Geochim. Cosmochim. Acta 121, 67–83.
Zhang, Y., 1998. The young age of Earth. Geochim. Cosmochim. Acta 62, 3185–3189.
Zhang, Y., 2002. The age and accretion of the earth. Earth Sci. Rev. 59, 235–263.
Zhang, Y., 2013. Superchondritic mantle is partially depleted mantle; and quantification of the spidergram sequence. 44th Lunar Planetary Science Conference. 18–22 March 2013 (abstract 1823).
Zhang, Y., 2014. Degassing history of Earth. Treatise of Geochem. 6, 37–69.
Zhang, Y., Zindler, A., 1989. Noble gas constraints on the evolution of Earth's atmosphere. J. Geophys. Res. 94, 13719–13737.
Zindler, A., Hart, S., 1986. Chemical geodynamics. Ann. Rev. Earth Planet. Sci. 14, 493–571.